Supramolecular Polymers

DOI: 10.1002/ange.200805680

STM Insight into Hydrogen-Bonded Bicomponent 1D Supramolecular Polymers with Controlled Geometries at the Liquid–Solid Interface**

Artur Ciesielski, Gaël Schaeffer, Anne Petitjean, Jean-Marie Lehn, and Paolo Samorì**

Self-assembly of molecular species into well-defined multicomponent supramolecular architectures[1] can be obtained by selective association of complementary building blocks undergoing molecular recognition events. Among weak interactions, hydrogen bonding offers a high level of control over the process of molecular self-assembly, since it combines reversibility, directionality, specificity, and cooperativity. It has in particular been implemented for the generation of supramolecular polymers[2] through the polyassociation of molecular components bearing complementary recognition groups. Supramolecular polymers can simultaneously display tunable material properties with low-viscosity melts.[3] Their mechanical features result especially from secondary interactions, in particular the strength, reversibility, and directionality of those interactions. Hitherto, H-bonded supramolecular architectures have been self-assembled on solid surfaces into highly ordered motifs, both under ultrahigh vacuum (UHV)[4] and at the solid–liquid interface.[5] Whereas for the former case the formation of multicomponent 1D H-bonded polymers was recently reported,[6] for the latter, the effort has to date been primarily devoted to H-bonded architectures consisting of multicomponent discrete assemblies[7] or to monocomponent 1D polymers.[8] The generation of ordered motifs stabilized by hydrogen bonds on a solid surface requires the fine tuning of the interplay between the interactions among neighboring molecules and the adsorbate–substrate interactions.[9] The controlled formation of ordered multicomponent architectures at the solid–liquid interface from a concentrated solution is thermodynamically unfavored. In fact, among the various components in the supernatant solution, the component with a greater affinity for the substrate, that is, offering a minimization of the free interface energy per unit area, will assemble on its surface, whereas the others will remain in solution.[10] To immobilize all the components on the surface, thus to achieve a complete physisorption of all the components at the solid–liquid interface, it is necessary to borrow a strategy commonly employed under UHV, that is, control of the stoichiometry of the molecules absorbed at surfaces.[11] At the solid–liquid interface, the number of molecules in the solution applied to the surface should be lower than that required to form a monolayer of physisorbed molecules lying flat on the basal plane of the substrate. However, operating under such conditions, that is, at low concentration, can lead to polymorphism.[12] Although the use of H-bonds to form bicomponent linear supramolecular polymers was introduced over 15 years ago,[2e–f] to date, visualization by scanning tunneling microscopy (STM) has not been explored at the liquid–solid interface for supramolecular polymers composed of two components interacting through multiple hydrogen bonds, leading to an architecture with a controlled geometry and, in principle, an infinite length. STM at the solid–liquid interface has been the method of choice for the visualization of monolayers as it offers detailed submolecular-scale insight into the self-assembly of organic molecules on surfaces and its evolution over time with millisecond resolution.[13]

Herein we present STM visualization at the liquid–solid interface at room temperature of the formation of supramolecular hydrogen-bonded polymers with either a linear or a zigzag geometry on highly oriented pyrolitic graphite (HOPG) surfaces. To this end, we used the ditopic molecular components **1**–**3** (Scheme 1), bearing complementary hydrogen-bonding recognition groups: either a Janus-type cyanuric wedge **2** or barbituric wedge **3** (ADA-ADA-array) and a corresponding (DAD-DAD-array) receptor unit **1**.[14] These molecules were selected because they are known to form 1D supramolecular polymeric strands in solution by polyassociation through sextuple hydrogen bonding between their respective recognition sites[15] (Figure 1).

Initially we investigated the homomolecular self-assembled structures obtained by applying a drop of a (6 ± 1) μM solution of the molecule **1**[16] in 1,2,4-trichlorobenzene (TCB) on the graphite surface. STM images of the obtained monolayer (Figure 2) show a polycrystalline structure with two different domains **A** and **B**, which coexist for a several minutes (see survey STM image in the Supporting Information, Figure SI3). The two crystals are characterized by a different packing motif. The assembly in domain **A** presents parallel lamellae (Figure 2a) and has the unit cell: $a=(1.78\pm0.2)$ nm, $b=(5.62\pm0.2)$ nm, $\alpha=(90\pm2)°$, corresponding to an area $A=(10.0\pm1.2)$ nm^2, given that each unit cell contains one molecule **1**. Given its size there is space enough to accommodate all the aliphatic side groups on the surface, although, since we have not resolved them, we do not have unambiguous confirmation of this aspect. It is interesting to

[*] A. Ciesielski, G. Schaeffer, Dr. A. Petitjean,[+] Prof. J.-M. Lehn, Prof. P. Samorì
ISIS/UMR CNRS 7006, Université Louis Pasteur
8 Allée Gaspard Monge, 67000 Strasbourg (France)
E-mail: lehn@isis.u-strasbg.fr
samori@isis-ulp.org

[+] Present address: Chemistry Department, Queen's University Kingston, ON, K7L 3N6 (Canada)

[**] This work was supported by the EU through the Marie Curie EST project SUPER (MEST-CT-2004-008128) and RTN PRAIRIES (MRTN-CT-2006-035810), as well as by the ERA-Chemistry project SurConFold, the Université Louis Pasteur and CNRS. A.C. and G.S. thank the French Ministry of Research for a predoctoral fellowship.

Supporting information for this article is available on the WWW under http://dx.doi.org/10.1002/anie.200805680.

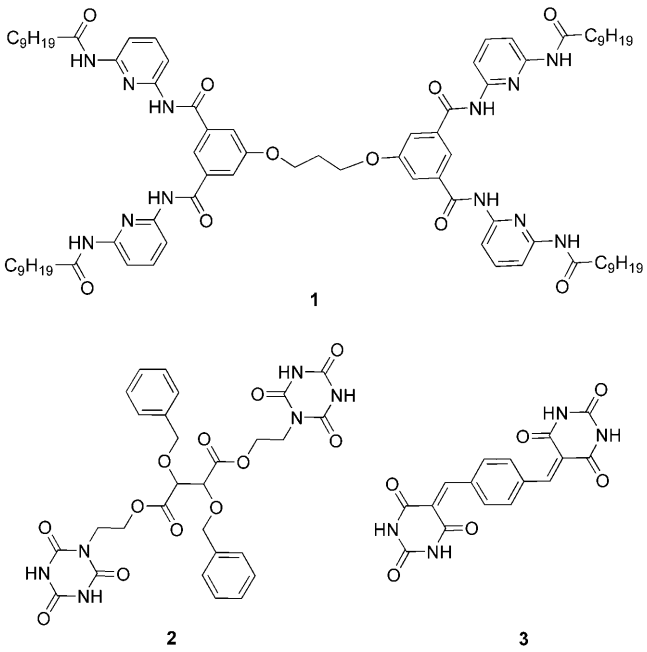

Scheme 1. Ditopic molecular components bearing hydrogen-bonding recognition groups.

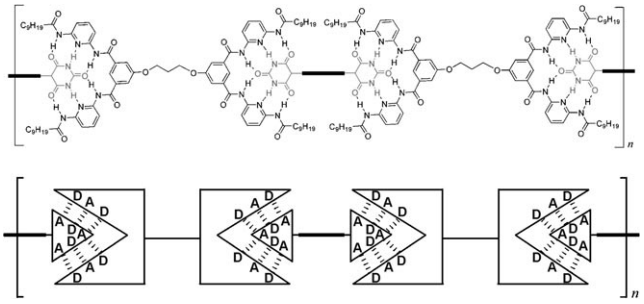

Figure 1. Formation of a main-chain supramolecular polymer by polyassociation of molecular monomers of type **1** and **2** or **3** through sextuple hydrogen bonding between their complementary recognition units.

point out that the lifetime of domain **A** was very short, that is, it disappeared after a few minutes, proving its metastable nature. The poor stability of domain **A** was also evidenced by its high molecular dynamics on a timescale comparable to that of the tip scanning. For this reason we have not been able to achieve a high submolecular resolution. Such poor stability is not surprising. For enthalpy reasons, the system is prone to form a densely packed assembly, thus minimizing the size of the unit cell. The more stable domain **B** features the unit cell: $a = (4.42 \pm 0.2)$ nm, $b = (5.65 \pm 0.2)$ nm, $\alpha = (90 \pm 2)°$, leading to an area $A = (24.9 \pm 1.4)$ nm^2, where each unit cell contains four molecules **1** (Figure 2b). Among them, one molecule (indicated by a white arrow) seems to be partially desorbed. Given the area of the darker spots in the STM image $A_{s1} = (11 \pm 2)$ nm^2 (see the Supporting Information), and by comparing it with the area occupied by a 2D projected C_9H_{19} chain ($A_{C_9H_{19}} = (0.33 \pm 0.02)$ nm^2), it is likely that all

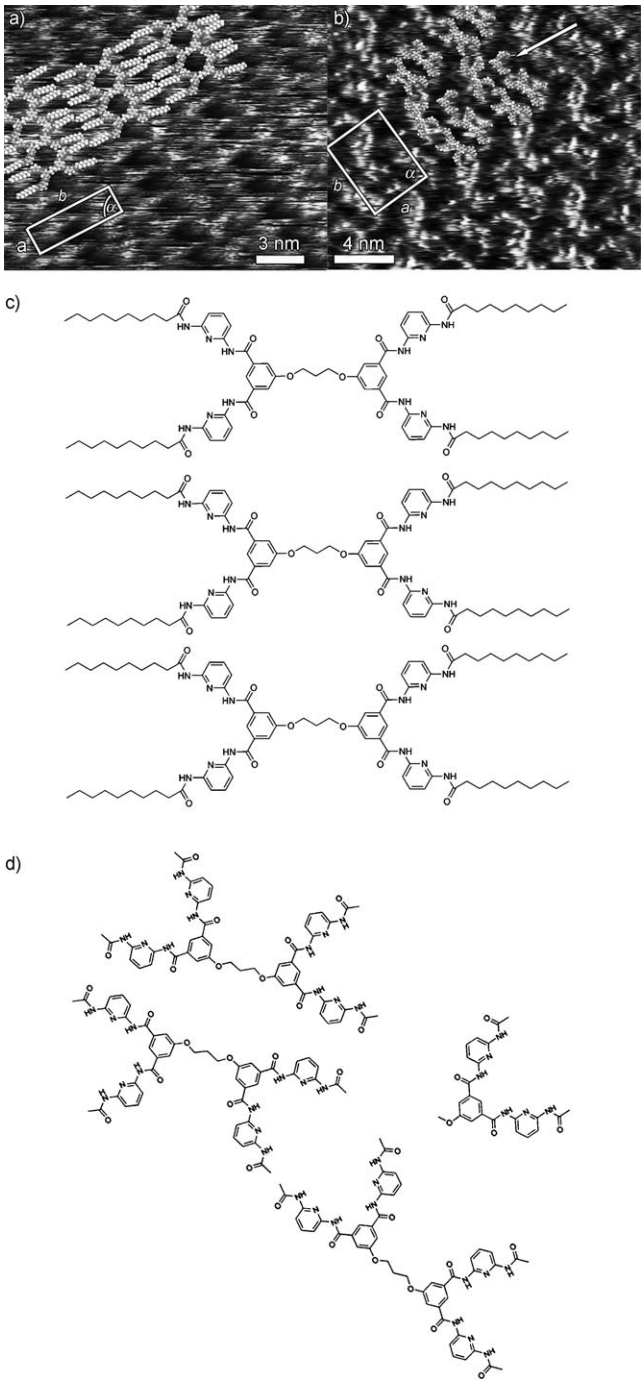

Figure 2. STM images of a monolayer of molecule **1** at the liquid-graphite interface self-assembled from a solution 1,2,4-trichlorobenzene: a) Domain **A**. Tunneling parameters: average tunneling current (I_t) = 0.5 pA, bias voltage (V_t) = 100 mV; b) domain **B**. Tunneling parameters: I_t = 15 pA, V_t = 300 mV; average area of the darker spots $A_{s1} = (11 \pm 2)$ nm^2; c) model of the molecular components in domain **A**; d) model of the molecular components in domain **B**.

fourteen nonyl side chains are physisorbed on the HOPG surface, although, owing to their highly dynamic nature, we are unable to resolve them.

We then extended our studies to heteromolecular noncovalently engineered main-chain supramolecular polymers resulting from self-assembly on graphite from a bicomponent

solution containing molecule **1**[16] and either molecule **2** or **3**.[17] It is important to note that molecule **1** was visualized at the HOPG–solution interface only upon using 1,2,4-trichlorobenzene (TCB) as solvent. Study of this system in different solvents, 1-phenyloctane and tetradecane, did not produced any ordered monolayers. For this reason, we continued our study using TCB as a solvent. Neither molecule **2** nor **3** were found to form ordered structures in single-component films at the liquid–solid interface, highlighting a low affinity for the graphite surface. The heteromolecular monolayer was formed by applying a 4 μL drop of the solution in TCB to the surface. The two bicomponent solutions were obtained by mixing 5–10 mM solutions of **1**+**2** or **1**+**3** in DMSO and subsequently diluting them with TCB, to yield concentrations of (4 ± 1) μM and (3 ± 1) μM for **1**+**2** and **1**+**3**, respectively. The procedure for the deposition of the two components on the surface is critical for the formation of the mixed polymer, as, if one partner molecule is already physisorbed on the surface, its partial desorption is energetically unfavorable, thereby hindering the emergence of molecular recognition leading to homogeneous intermixing on the substrate surface. Therefore both **1**+**2** and **1**+**3** solutions were prepared ex situ. Notably, the formation of bicomponent polymers was visualized only when the ratio of the concentrations of the molecules was (30 ± 5)% of molecule **1** to (70 ± 5)% of molecule **2** and **3**.

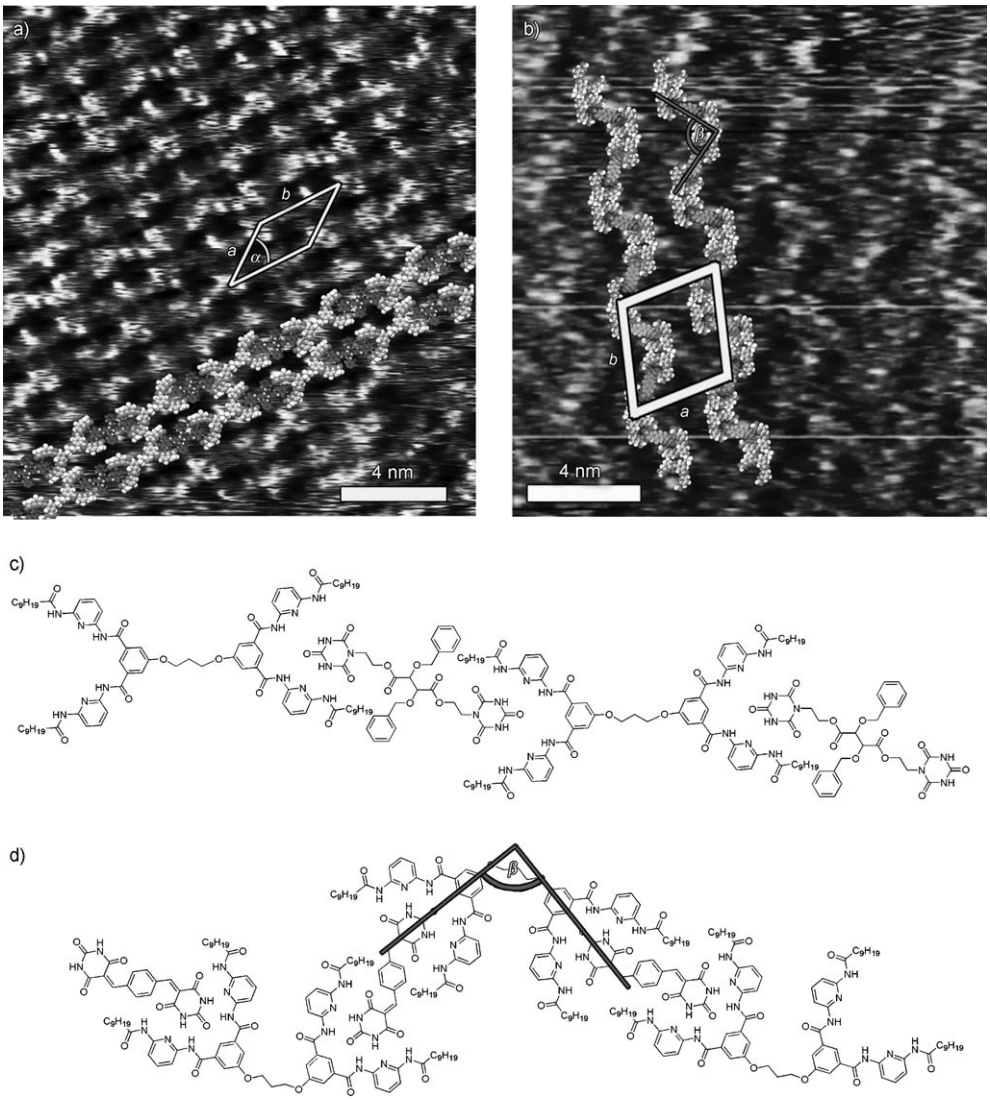

Figure 3. STM images of monolayers of linear bicomponent supramolecular H-bonded polymer at the liquid–graphite interface self-assembled from TCB solution; a) linear structure of polymer **1**+**2**; area of darker spots $A_s=(1.3\pm2)$ nm^2. Tunneling parameters: $I_t=20$ pA, $V_t=300$ mV; b) self-assembled bicomponent polymer **1**+**3**; the area of the darker spots $A_s=(4\pm1)$ nm^2. Tunneling parameters: $I_t=20$ pA, $V_t=300$ mV; c) linear polymer **1**+**2**; d) linear polymer **1**+**3**.

By decreasing the concentration of molecules **2** and **3** or increasing the concentration of molecule **1**, only patterns of molecule **1** were seen on the HOPG surface. This observation confirms the greater affinity of molecule **1** for the graphite surface.

Figure 3a shows a STM image of the linear heteromolecular polymer resulting from deposition of a mixture of molecules **1** and **2**. The monolayer displays a polycrystalline structure, which consists of tens of nanometer-wide domains that are stable over several minutes. The proposed packing motif is in excellent agreement with that suggested by modeling (Figure 1). The symmetric molecule **1** forms six hydrogen bonds with each neighboring molecule **2**. The formation of a linear architecture is made possible especially taking advantage of the conformational flexibility of the cyanuric wedge **2**. The core of each molecule is physisorbed flat on the surface. The unit cell parameters, $a=(2.72\pm0.2)$ nm, $b=(3.45\pm0.2)$ nm, and $\alpha=(35.8\pm2)°$, lead to an area $A=(5.5\pm0.6)$ nm^2/dimer, where each unit cell contains one molecule **1** and one molecule **2** (Figure 3a). The proposed supramolecular motif, featuring a bicomponent linear association **1**+**2** (Figure 3c), matches the pattern observed in the STM image, ruling out the presence of the energetically equivalent armchair-based motif. Deposition of a small amount (ca. 4 μL) of molecule **1** and of the bridging molecule

3 in a 3:7 stoichiometry results also in the formation of a 1D heteromolecular polymer. However, differently from the linear motif observed for **1** + **2**, the bicomponent supramolecular polymer has an intralamellar zigzag geometry. The angle β between the two adjacent molecular units in the 1D supramolecular polymer is $(90 \pm 2)°$. This change in packing can be ascribed to the greater rigidity of molecule **3** compared to **2**. To enable heteromolecular association of two edges, molecule **1** needs to adopt a bent conformation, which is possible thanks to a flexible central -OC_3H_6O- moiety. The distance between the two parallel lamellae, that is, between two adjacent bright structures in the STM image, corresponds to the length of the C_9H_{19} chains, indicating that, in this case, all the C_9H_{19} chains of molecule **1** are physisorbed on the HOPG surface. However, owing to dynamics on a faster timescale than the tip scanning, we were not able to resolve them (Figure 3b). The darker areas in the STM current images (Figure 3a and b) were estimated and compared with the space that would be occupied by the nonyl chains physisorbed on the graphite. These areas were found to be $A_{\mathbf{s1+2}} = 0.85\ nm^2$ and $A_{\mathbf{s1+3}} = 2.45\ nm^2$ for **1** + **2** and **1** + **3** respectively, whereas the modeled area occupied by each C_9H_{19} chain amounts to $A_{C_9H_{19}} = (0.33 \pm 0.02)\ nm^2$, which suggests that, for the monolayer of **1** + **2**, most of the chains are backfolded in the supernatant solution, whereas for **1** + **3** they are packed on the surface. The unit cell parameters for **1** + **3** are $a = (3.93 \pm 0.2)$ nm, $b = (4.27 \pm 0.2)$ nm, $\alpha = (75 \pm 2)°$, $A = (16.2 \pm 1.2)\ nm^2$/dimer. Each unit cell contains two molecules **1** and two molecules **3** (Figure 3a). In the proposed packing model of the bicomponent linear polymer **1** + **3** (Figure 3d) each molecule **1** forms six hydrogen bonds with each neighboring molecule **3**.

In summary, by working at a low concentration, in experimental conditions not susceptible to thermodynamically driven phase segregation between two components on the solid–liquid interface, we have been able for the first time to visualize, by STM on the molecular scale, the physisorption of 1D main-chain bicomponent H-bonded supramolecular polymers at surfaces, owing to appropriate design of complementary building blocks linked by the formation of six H-bonds at each node. By using two different connecting molecules, **2** and **3**, featuring different conformational rigidity, we were able to control the geometry of the linear supramolecular polymer. When a flexible component was used to bridge adjacent molecules of **1**, a linear structure was obtained, whereas when the bridging molecule was rigid, a zigzag motif was observed. The visualization of bicomponent supramolecular polymers at the liquid–solid interface paves the way towards the understanding of the mechanism of their formation on surfaces.[3] It also adds further weight to the initial concept of supramolecular polymers and supramolecular polymer chemistry,[2e–f,18] that has been widely implemented, in particular in bulk materials.[2a–d] Furthermore, the generation of rigid bicomponent supramolecular polymers, such as **1** + **3**, which present a controlled curvature at the liquid–solid interface represents the first step towards the nanopatterning of surfaces with multicomponent functional architectures for exploitation of vectorial properties. The introduction of cross-linking components[15] may allow extension into 2D supramolecular assemblies.

Received: November 20, 2008
Revised: December 21, 2008
Published online: January 29, 2009

Keywords: interfaces · polymers · scanning probe microscopy · self-assembly · supramolecular chemistry

[1] J.-M. Lehn, *Supramolecular Chemistry: Concepts and Perspectives*, VCH, New York, **1995**.
[2] a) *Supramolecular Polymers*, 2nd ed. (Ed.: A. Ciferri), Taylor & Francis, Boca Raton, FL, **2005**; b) L. Brunsveld, B. J. B. Folmer, E. W. Meier, R. P. Sijbesma, *Chem. Rev.* **2001**, *101*, 4071; c) J.-M. Lehn, *Polym. Int.* **2002**, *51*, 825; d) J.-M. Lehn, *Prog. Polym. Sci.* **2005**, *30*, 814; e) C. Fouquey, J.-M. Lehn, A.-M. Levelut, *Adv. Mater.* **1990**, *2*, 254; f) T. Gulik-Krzywicki, C. Fouquey, J.-M. Lehn, *Proc. Natl. Acad. Sci. USA* **1993**, *90*, 163.
[3] T. F. A. de Greef, E. W. Meijer, *Nature* **2008**, *453*, 171.
[4] a) J. V. Barth, *Annu. Rev. Phys. Chem.* **2007**, *58*, 375; J. V. Barth, G. Costantini, K. Kern, *Nature* **2005**, *437*, 671; b) F. Rosei, M. Schunack, Y. Naitoh, P. Jiang, A. Gourdon, E. Laegsgaard, I. Stensgaard, C. Joachim, F. Besenbacher, *Prog. Surf. Sci.* **2003**, *71*, 95.
[5] S. De Feyter, F. C. De Schryver, *Chem. Soc. Rev.* **2003**, *32*, 139.
[6] a) A. Llanes-Pallas, M. Matena, T. Jung, M. Prato, M. Stöhr, D. Bonifazi, *Angew. Chem.* **2008**, *120*, 7840; *Angew. Chem. Int. Ed.* **2008**, *47*, 7726; b) M. E. Cañas-Ventura, W. Xiao, D. Wasserfallen, K. Müllen, H. Brune, J. V. Barth, R. Fasel, *Angew. Chem.* **2007**, *119*, 1846; *Angew. Chem. Int. Ed.* **2007**, *46*, 1814.
[7] a) S. De Feyter, A. Miura, S. Yao, Z. Chen, F. Würthner, P. Jonkheijm, A. P. H. J. Schenning, E. W. Meijer, F. C. De Schryver, *Nano Lett.* **2005**, *5*, 77; b) K. Eichhorst-Gerner, A. Stabel, G. Moessner, D. Declerq, S. Valiyaveettil, V. Enkelmann, K. Müllen, J. P. Rabe, *Angew. Chem.* **1996**, *108*, 1599–1602; *Angew. Chem. Int. Ed. Engl.* **1996**, *35*, 1492; c) A. Miura, Z. J. Chen, H. Uji-i, S. De Feyter, M. Zdanowska, P. Jonkheijm, A. Schenning, E. W. Meijer, F. Würthner, F. C. De Schryver, *J. Am. Chem. Soc.* **2003**, *125*, 14968; d) W. Mamdouh, R. E. A. Kelly, M. D. Dong, L. N. Kantorovich, F. Besenbacher, *J. Am. Chem. Soc.* **2008**, *130*, 695; e) S. De Feyter, M. Larsson, A. Gesquière, H. Verheyen, F. Louwet, B. Groenendaal, J. van Esch, B. L. Feringa, F. De Schryver, *ChemPhysChem* **2002**, *3*, 966; f) F. Cicoira, C. Santato, F. Rosei, *Top. Curr. Chem.* **2008**, *285*, 203; g) K. G. Nath, O. Ivasenko, J. A. Miwa, H. Dang, J. D. Wuest, A. Nanci, D. F. Perepichka, F. Rosei, *J. Am. Chem. Soc.* **2006**, *128*, 4212.
[8] a) G. Gottarelli, S. Masiero, E. Mezzina, S. Pieraccini, J. P. Rabe, P. Samorì, G. P. Spada, *Chem. Eur. J.* **2000**, *6*, 3242; b) A. Gesquière, M. M. S. Abdel-Mottaleb, S. De Feyter, F. C. De Schryver, F. Schoonbeek, J. van Esch, R. M. Kellogg, B. L. Feringa, A. Calderone, R. Lazzaroni, J. L. Brédas, *Langmuir* **2000**, *16*, 10385; c) C. Meier, U. Ziener, K. Landfester, P. Weihrich, *J. Phys. Chem. B* **2005**, *109*, 21015; d) H. Zhou, H. Dang, J. H. Yi, A. Nanci, A. Rochefort, J. D. Wuest, *J. Am. Chem. Soc.* **2007**, *129*, 13774; e) G. P. Spada, S. Lena, S. Masiero, S. Pieraccini, M. Surin, P. Samorì, *Adv. Mater.* **2008**, *20*, 2433.
[9] J. P. Rabe, S. Buchholz, *Science* **1991**, *253*, 424.
[10] C. A. Palma, M. Bonini, T. Breiner, P. Samorì, *Adv. Mater.* **2009**, DOI: 10.1002/adma.200802068.
[11] C. A. Palma, M. Bonini, A. Llanes-Pallas, T. Breiner, M. Prato, D. Bonifazi, P. Samorì, *Chem. Commun.* **2008**, 5289.
[12] a) S. Lei, K. Tahara, F. C. De Schryver, M. van der Auweraer, Y. Tobe, S. De Feyter, *Angew. Chem.* **2008**, *120*, 3006; *Angew.*

Chem. Int. Ed. **2008**, *47*, 2964; b) L. Kampschulte, T. L. Werblowsky, R. S. K. Kishore, M. Schmittel, W. M. Heckl, M. Lackinger, *J. Am. Chem. Soc.* **2008**, *130*, 8502.
[13] a) S. De Feyter, F. C. De Schryver, *J. Phys. Chem. B* **2005**, *109*, 4290; b) M. Surin, P. Samorì, *Small* **2007**, *3*, 190.
[14] a) S. K. Chang, D. Van Engen, E. Fan, A. D. Hamilton, *J. Am. Chem. Soc.* **1991**, *113*, 7640; b) S. K. Chang, A. D. Hamilton, *J. Am. Chem. Soc.* **1988**, *110*, 1318.
[15] V. Berl, M. Schmutz, M. J. Krische, R. G. Khoury, J.-M. Lehn, *Chem. Eur. J.* **2002**, *8*, 1227.
[16] E. Kolomiets, E. Buhler, S. J. Candau, J. M. Lehn, *Macromolecules* **2006**, *39*, 1173.
[17] a) Z. Wang, L. Wang, X. Zhang, J. Shen, S. Denzinger, H. Ringsdorf, *Macromol. Chem. Phys.* **1997**, *198*, 573; b) B. S. Jursic, E. D. Stevens, *Tetrahedron Lett.* **2003**, *44*, 2203.
[18] J.-M. Lehn, *Makromol. Chem. Macromol. Symp.* **1993**, *69*, 1.

